regeneratoren, Z. *Angew. Math. Mech.* 3, 173–200 (1929).
8. A. J. Willmott and R. J. Thomas, Analysis of the long contra-flow regenerative heat exchanger, *J. Inst. Math. Applic.* 14, 267–280 (1974).
9. H. Hausen, Vervollstandigte Berechnung des Wärmeaustauches in Regeneratoren, *Z. Ver. Dt. Ing, Beihelft Verftk* 2, 31–43 (1942).
10. D. R. Hartree, *Numerical Analysis*, p. 114. Oxford University Press, Oxford (1958).

Int. J. Heat Mass Transfer. Vol. 22, pp. 973–976

0017-9310/79/0601-0973 $02.00/0

MEASUREMENT OF BOILING CURVES DURING REWETTING OF A HOT CIRCULAR DUCT

W. J. CHEN,* Y. LEE* and D. C. GROENEVELD†

(*Received* 16 *January* 1978 *and in revised form* 30 *November* 1978)

NOMENCLATURE

c_p, specific heat at constant pressure [J/kg K];
D, diameter [m];
G, mass flow rate [g/m^2 s];
h, heat-transfer coefficient [W/m^2 K];
i, enthalpy [J/kg];
k, thermal conductivity [W/m K];
Q, heat [W];
q'', heat flux [W/m^2];
q''', heat generation rate [W/m^3];
T, temperature [°C];
t, time;
U, rewetting velocity [m/s];
w, flow rate [kg];
z, length [m];
ρ, density [kg/m^3].

Subscripts

a, heat conducted axially;
ac, heat convected to the coolant;
el, electrical heat generation;
i, inside;
in, inlet;
ls, heat loss to surroundings;
o, outside;
p, peripheral;
q, quenching;
rd, net radiation from the wall to the coolant;
sat, saturation;
w, wall;
wi, wall inside;
wo, wall outside;
z, elevation.

INTRODUCTION

THE PRESENT study was designed to investigate transient heat-transfer modes which can be encountered during reflooding of a reactor core following a loss-of-coolant accident. Previous reflooding studies have concentrated on (i) developing analytical models for reflooding [1–3] which are based on assumptions regarding heat-transfer coefficients on the wet and dry side, and (ii) experimental studies which were mainly concerned with measurement of rewetting velocities and wall temperature–time gradients [4]. The contribution of this study is that it presents experimentally derived boiling curves obtained during reflooding tests over a wide range of experimental parameters.

*Department of Mechanical Engineering, University of Ottawa, Ottawa, Canada K1N 6N5.
†Atomic Energy of Canada Limited, Chalk River, Ontario, Canada K0J 1J0.

EXPERIMENT

The experimental loop consisted of the following components in series: demineralizer, preheater, boiler, pump, flowmeter, test section with parallel bypass, and condenser. Three test sections were used in this investigation; details are presented in Table 1.

Each test section was instrumented with about forty chromel–alumel thermocouples, spot-welded onto the outside wall surface at different axial and peripheral positions. The test sections were heated by a 30 kVA, 1500 amp AC power supply and were well insulated. The terminal clamps, made of copper, were attached to both ends of the test section. Pressure transducers were used for monitoring test section inlet and outlet pressure. Further details are given in [5].

All tests were conducted using water at atmospheric pressure, with the following ranges of test parameters: flow rate 10–40 g cm^{-2} s^{-1}, initial wall temperature 270–800°C, inlet subcooling 10–80°C, test section power 0–20 kW. At the start of each test the power to the test section was turned on and the wall temperature was brought up to the desired value. Experiments were performed by diverting the water flow from the bypass circuit, to the test section while the power was either maintained or switched off, depending on the selection of the test parameters. The signals from the thermocouples, and from the transducers (for flow rate, pressures, and power to the test section) were recorded and printed out simultaneously.

DATA REDUCTION

The rewetting velocities and the average initial wall temperatures were derived from the temperature–time traces using the method commonly used by other investigators [6, 7].

The surface heat flux to the coolant may be extracted from the data by using the energy balance for the length ΔZ of the test section shown in Fig. 1

$$\frac{dQ}{dt} = Q_{el} - Q_c - Q_a - Q_{rd} - Q_{ls}. \quad (1)$$

It is assumed here that the axial conduction heat flux may be approximated by a one-dimensional conduction model. Justification will be provided in the discussion section.

Table 1. Physical characteristics of test sections

Test Section No.	1	2	3
Material	S.S. 304	S.S. 304	Inconel X-750
Tube O.D., mm	19.1	19.1	15.9
Tube wall thickness, δ, mm	1.65	0.89	1.02
Tube length, approx., m	4	3.5	3.5

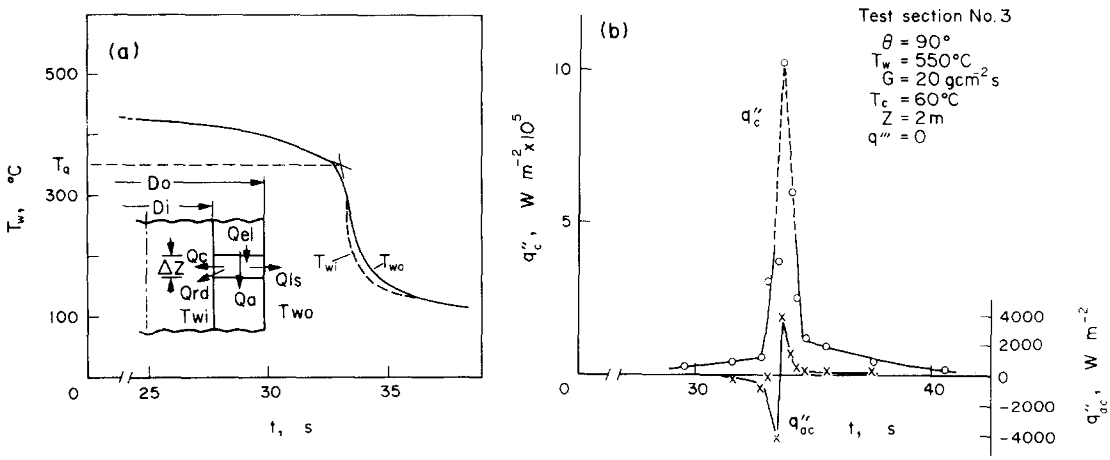

FIG. 1. Temperature transient and corresponding heat flux transient during rewetting of a hot tube.

Based on this assumption, Q_a may then be approximated to be

$$\frac{\pi}{4}(D_o^2-D_i^2)\frac{k}{U^2}\frac{d^2T_w}{dt^2}\Delta z$$

using the relationship

$$\frac{dT_w}{dz}=\frac{1}{U}\frac{dT_w}{dt}.$$

It has been shown by Thompson that $U \neq f(z)$.

Q_{rd} is significant at high wall superheats but is less than 1% of the total heat flux near the quench front. Therefore, it is neglected in the present study. $Q_{ls} = q_{ls}''T_w\pi D_o\Delta z$, was obtained from calibration tests.

After substitution with appropriate values and with above assumptions, equation (1) becomes

$$q_c''=\frac{D_o^2-D_i^2}{4D_i}\left(q'''-(\rho Cp)_w\cdot\frac{dT_w}{dt}-\frac{k}{U^2}\frac{d^2T_w}{dt^2}\right)-q_{ls}''(T_w)\frac{D_o}{D_i}. \quad (2)$$

The above equation can be evaluated using the measured values of dT_w/dt. Strictly speaking dT_w/dt should be averaged across the wall, but the difference in dT_{w_o}/dt (evaluated at the outside) and dT_{w_i}/dt (at the inside) is small. T_{w_i} and dT_{w_i}/dt were evaluated using the solution to the inverse heat-transfer problem [9]. Finally, the inside heat-transfer coefficient can be evaluated from $h = \ddot{q}_c''/(T_{w_i} - T_{sat})$.

RESULTS AND DISCUSSIONS

During the reflooding period, several heat-transfer modes occur successively at a given location, resulting in a continuous change of the surface heat flux. Parameters, which can influence the heat-transfer rate include coolant flow rate, coolant inlet subcooling, initial wall temperature, wall thickness, wall material and axial location.

Figure 1(b) shows the variation of surface heat flux, q_c'', with time for a given test condition as evaluated from equation (2). The contribution of axial conduction to the surface heat flux, q_{ac}, is also shown.* As can be seen, its effect is significant. The maximum boiling heat-transfer coefficients in the wet-region obtained in the present experimental study are always an order or two smaller than those predicted [6, 8]. Possible incorrect assumptions of heat-transfer correlations for nucleate boiling, film boiling and rewetting temperatures may have been responsible for their high values of heat-transfer coefficient and Biot numbers. Their conclusion that axial conduction is very significant and thus a two-dimensional model must be used, is contrary to our findings.

EFFECT OF AXIAL LOCATION

The local liquid subcooling decreases along the length of the test section. This decrease depends on the coolant flow rate and heat-transfer rate from the wall. For the experimental conditions shown in Fig. 2(a), the coolant temperature upstream of the rewetting front increases about 2°C/m along the channel. Therefore, no significant effect of axial location on surface heat flux in the nucleate boiling region could be expected as is shown in the figure.

However, the critical heat flux and the surface heat flux in the transition boiling region decrease with increasing axial distance from the inlet along the test section. This could be partially attributed to the increased distance from the inlet and the reduced local subcooling, which both have a negative effect on critical heat flux.

EFFECT OF INITIAL WALL TEMPERATURE

The convective heat-transfer coefficient is mainly affected by the change in flow conditions. As a result, the film boiling heat flux is almost independent of wall superheat as shown in Fig. 2(b). But a higher initial wall temperature means that more time is required to remove the stored heat from the wall. Hence the rewetting velocity will be lower and the "apparent quenching temperature" [T_q, Fig. 1(a)]

$$*q_{ac}''=\frac{D_o^2-D_i^2}{4D_i}\cdot\frac{k}{U^2}\frac{d^2T_w}{dt^2}.$$

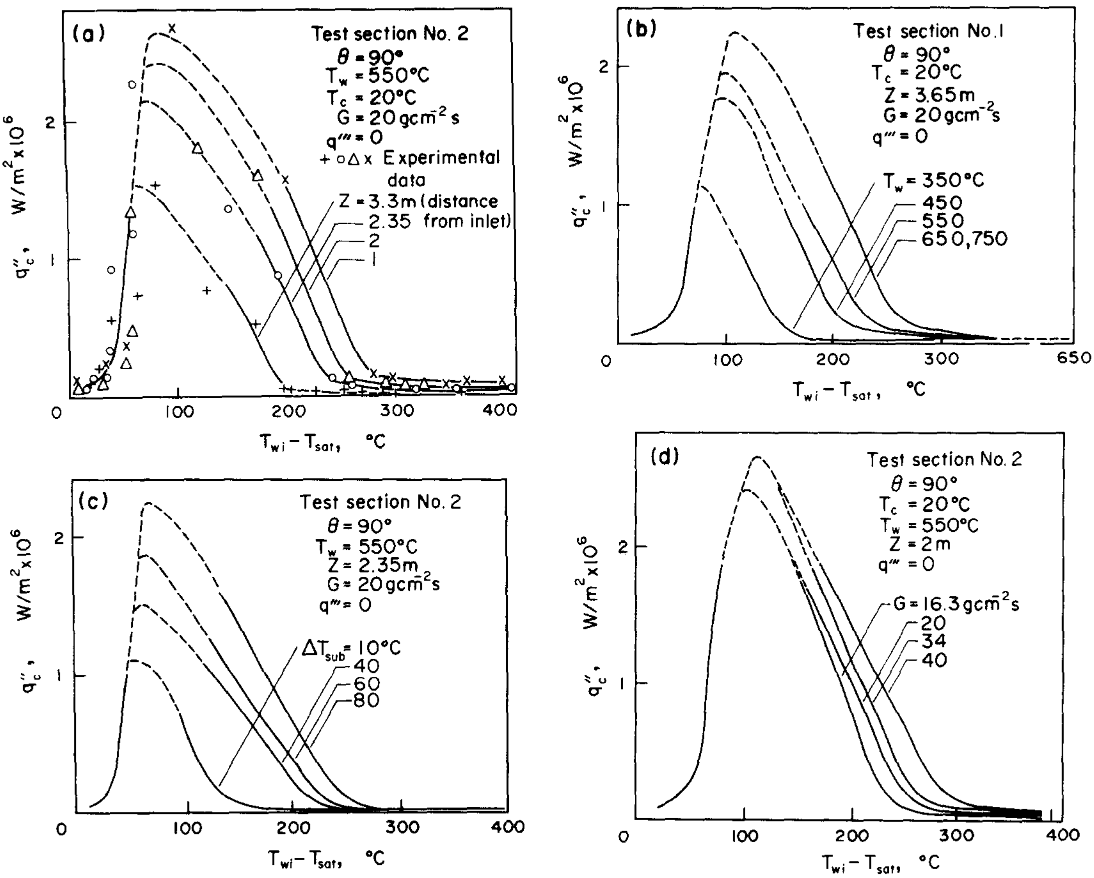

FIG. 2. Parametric effects on boiling curve of (a) axial location; (b) initial wall temperature; (c) inlet subcooling, and (d) mass flux.

higher [10]. It was observed that once the initial wall temperature exceeds 650°C, the apparent quench temperature remains almost constant. In this case, the surface heat flux is independent of the initial wall temperature.

EFFECT OF COOLANT SUBCOOLING

Figure 2(c) shows that for all heat-transfer modes encountered, the surface heat flux increases with coolant subcooling. However, the difference in the film boiling heat fluxes is relatively small.

The rewetting velocity also increased at higher inlet subcooling. This was expected as a higher inlet subcooling increases the film boiling heat flux significantly [11]. The resulting reduction in dry wall temperature will permit a more rapid propagation of the rewetting front. In addition, subcooling also increases the CHF and the transition boiling heat flux thus improving the axial conduction heat transfer process and permitting a further increase in rewetting velocity.

EFFECT OF FLOW RATE

For subcooled boiling a higher flow rate increases the film boiling, transition boiling and critical heat flux [11]. This will result in an increase of rewetting velocity as was shown above. A higher flow rate will also reduce the coolant enthalpy rise which will further increase the rewetting velocity. A strong positive effect of flow rate on rewetting velocity was indeed observed. Figure 2(a) shows that the critical heat flux and surface heat flux in the transition boiling and film boiling region increase slightly with the coolant flow rate. The increase in post-CHF heat transfer is expected, since convective heat transfer increases with increasing coolant flow rate, resulting in a higher heat transfer coefficient for the film boiling region.

EFFECT OF WALL THICKNESS

For the same initial and inlet conditions, the boiling curve derived from the two stainless steel test section results agree closely. This is expected as the convective heat-transfer phenomenon should not be affected by the change of wall thickness. The difference in heat storage capacity due to the increased wall thickness should affect the degree of subcooling at the quench front, but a calculation showed that this is negligible. With an increase in wall thickness, more heat must be removed from dry region to wet region of the rewetting front. Subsequently, the rewetting velocity tends to decrease with increasing wall thickness, as predicted by the simple one-dimensional analysis.

CONCLUSION

(1) Due to the high axial temperature gradient at the rewetting front, heat is transferred from dry region to wet region and successively released to the coolant in the nucleate boiling region. However, the contribution of axial conduction to the surface heat flux based on a one-dimensional conduction analysis is found to be small.

(2) The effective heat-transfer coefficients predicted by theoretical analysis of Thompson [1] and Yamanouchi [6] are an order or two larger than that obtained from these experiments.

(3) The film boiling heat flux increases with decreasing distance from inlet and with increasing coolant flow rate and subcooling. The transition boiling heat flux is mainly affected by the local coolant subcooling. No significant effect of coolant subcooling and flow rate on the nucleate boiling heat flux is observed.

REFERENCES

1. T. S. Thompson, An analysis of the wet-side heat transfer coefficient during rewetting of a hot dry patch, *Nucl. Engng Design* **22**, 212–224 (1972).
2. M. W. E. Coney, Calculation on the rewetting of hot surfaces, *Nucl. Engng Design* **31**, 246–259 (1974).
3. K. H. Sun, G. E. Dix and C. L. Tien, Effect of precursory cooling on falling-film rewetting, *J. Heat Transfer* **97**, 360–365 (1975).
4. F. F. Cadek, D. P. Dominicis and R. H. Leyse, PWR-FLECHT, final report, WCAP-7665, Westinghouse Electric Co., Pittsburgh (1971).
5. W. E. S. Gamblin and Y. Lee, The design of an experimental apparatus to measure transient post dryout heat transfer, Dept. of Mech. Engng, University of Ottawa (February 1976).
6. A. Yamanouchi, *J. Nu ci. Technol.* **5**, 547–558 (1968).
7. R. Martini and A. Prem ., *Energia Nucleare* **20**, 540–553 (1973).
8. T. S. Thompson, On the process of rewetting a hot surface by a falling liquid film, AECL-4516 (1973).
9. O. R. Burggraf, *J. Heat Transfer* **86**, 373–382 (1964). *J. Heat Transfer* **86**, 373–382 (1964).
10. Y. Lee, W. J. Chen and D. C. Groeneveld, Rewetting of very hot vertical and horizontal channels by flooding, in *Proceedings of the 6th International Heat Transfer Conference*, Toronto, 9–11 Aug. Vol. 5, pp. 95–100 (1978).
11. D. C. Groeneveld and K. K. Fung, Forced convective transition boiling, review of literature and comparison of prediction methods, AECL-5543 (1976).

Int. J. Heat Mass Transfer. Vol. 22, pp. 976–979
Pergamon Press Ltd. 1979. Printed in Great Britain

STUDY OF PRETRANSITIONAL INDUCED BENARD CONVECTION BY TWO-DIMENSIONAL NUMERICAL EXPERIMENTS

J. C. Legros,* J. Wesfreid† and J. K. Platten‡

(*Received* 18 *October* 1978)

NOMENCLATURE

Pr, Prandtl number ($Pr \equiv \nu/\kappa$);
Ra, Rayleigh number;
Ra^{cr}, critical value of Rayleigh number;
$\tilde{V}$, convective velocity;
V_0, velocity amplitude at $\varepsilon = 1$;
V_P, triggering velocity;
V_Z, vertical component velocity;
X, coordinate in the horizontal plate;
Z, coordinate in the vertical plate.

Greek symbols

ε, reduced deviation of the Rayleigh number to the critical one [$\varepsilon \equiv (Ra - Ra^{cr})/Ra^{cr}$];
θ, temperature perturbation amplitude;
ν, kinematic viscosity;
ξ, characteristic length;
τ, characteristic time;
Φ, vorticity;
Ψ, stream function.

1. INTRODUCTION

In a recent paper Wesfreid *et al.* [1] observed the induction of subcritical, space damped rolls by a triggering velocity applied to one side of a fluid layer maintained in controlled subcritical conditions, i.e. $\varepsilon = (Ra - Ra^{cr})/Ra^{cr} < 0$.

They compare their results with the Landau model expressed as:

$$\tau_0 \frac{\partial \tilde{V}}{\partial t} = \varepsilon \tilde{V} - \frac{\tilde{V}^3}{V_0^2} + \xi_0^2 \frac{\partial^2 \tilde{V}}{\partial X^2}, \tag{1}$$

where τ_0 and ξ_0 are the characteristic time and length respectively. V_0 is the velocity amplitude at $\varepsilon = 1$. At the stationary state for slow velocities [$\tilde{V}^3/(V_0^2|\varepsilon|) < 1$], the solution of the linearized equation (1) is

$$\tilde{V}(X) = V_P \exp - X/\xi^-, \tag{2}$$

with $\xi^- = \xi_0|\varepsilon|^{-0.5}$. V_P is the triggering velocity and

$$\lim_{x \to \infty} \tilde{V} = 0.$$

They verified this spatial exponential decay for the horizontal component of the velocity amplitude, V_X, of the induced rolls. They obtained a critical influence length $\xi^- = 0.378d|\varepsilon|^{-0.505}$ in very good agreement with the theoretically expected law: $\xi^- = 0.385d|\varepsilon|^{-0.5}$.

2. DESCRIPTION OF THE NUMERICAL EXPERIMENT

Recently Legros and Platten [2] gave new numerical results on nonlinear study of temperature and velocity distributions in the two-dimensional Bénard problem. This numerical approach has the particularity to simulate a Bénard apparatus of a given aspect ratio L/d with four rigid boundaries into which the number of convective cells is not imposed. The horizontal rigid boundaries are infinitely heat conductive and there is no heat flux through the lateral ones.

In this paper, we present results obtained with the finite differences method used in [2], for the study of pre-transitional induced Bénard convection. The dimensionless equations to be integrated are the conservation laws of momentum and of energy for a Boussinesq fluid of Prandtl number $Pr = 0.1$ in an apparatus of aspect ratio = 10.0. These equations are written as:

$$Pr \frac{\partial \Phi}{\partial t} = Pr \frac{\partial(\Psi, \Phi)}{\partial(X, Z)} - Ra \frac{\partial \theta}{\partial X} + Pr \nabla^2 \Phi, \tag{3}$$

$$Pr \frac{\partial \theta}{\partial t} = Pr \left[\frac{\partial(\Psi, \theta)}{\partial(X, Z)} - \frac{\partial \Psi}{\partial X} \right] + \nabla^2 \theta, \tag{4}$$

$$\Phi = \nabla^2 \Psi \tag{5}$$

*Université Libre de Bruxelles, Faculté des Sciences Appliquées, 50, avenue F.D. Roosevelt, B-1050, Bruxelles, Belgique.
†C. E. A. Saclay, D.Ph., Service de Physique du Solide et de Résonance Magnétique, B.P. n° 2, F-91190, Gif-Sur-Yvette, France.
‡Université de Mons, Faculté des Sciences, Avenue Maistriau, 21, B-7000, Mons, Belgique.